An insight, at the atomic level, into the structure and catalytic properties of the isomer Cu_{22} cluster

Huimin Zhou,[‡,a] Tao Yang,[‡,a] Huijuan Deng,[‡,a] Yapei Yun,[a] Shan Jin,[*,a] Lin Xiong,[*,b] Manzhou Zhu[*,a]

a. Key Laboratory of Structure and Functional Regulation of Hybrid Materials, Anhui University, Ministry of Education, Institutes of Physical Science and Information Technology, Anhui University, Department of Chemistry and Center for Atomic Engineering of Advanced Materials, Anhui University, Hefei, Anhui 230601, P. R. China.

b. School of Food and Chemical Engineering, Shaoyang University, Shaoyang 422000, PR China

1.1 Chemicals Materials

Copper tetraacetonitrile tetrafluoroborate ($Cu(CH_3CN)_4 \cdot BF_4$), 98.3%, Sigma-Aldrich), tris (4-fluorophenyl) phosphine (($P(Ph\text{-}^4F)_3$) ,99.7 % , Sigma-Aldrich), phenylselenol (C_6H_5SeH, 96 %, Sigma-Aldrich), sodium borohydride ($NaBH_4$, 98%, Sigma-Aldrich), acetonitrile (CH_3CN, HPLC, Aldrich), chloroform ($CHCl_3$, HPLC grade, Aldrich) n-hexane (Hex, HPLC grade, Aldrich), dichloromethane (CH_2Cl_2, HPLC grade, Aldrich). All reagents were used as received without further purification.

1.2 The synthesis of isomer Cu_{22} clusters

Typically, cooper salt ($Cu(CH_3CN)_4 \cdot BF_4$, 160 mg, 0.51 mmol) was added to the mixed solution of 5ml acetonitrile and 5ml chloroform under vigorous stirring. After 10 mins, tris (4-fluorophenyl) phosphine ($P(Ph\text{-}^4F)_3$), 116 mg, 0.367mmol) and phenylselenol (C_6H_5SeH, 23μl, 0.146 mmol) were added together to the mixed solution. After 15 min, a freshly prepared solution of sodium borohydride (60 mg, in 2 ml CH_3OH) was added. The reaction lasted for 4h at room temperature. The crude product was obtained by removing the excess solution with a rotary evaporator. The isomers $Cu_{22}(SePh)_{10}(Se)_6((P(Ph\text{-}^4F)_3)_8)$ were crystallized in a mixture of CH_2Cl_2 and n-hexane at room temperature for 2 weeks. Black block and yellow flake crystals were observed, which were identified as Cu_{22}-1 and Cu_{22}-2, respectively.

1.3 Characterization

X-ray photoelectron spectroscopy (XPS) measurements were performed on a Thermo ESCALAB 250 configured with a mono chromated AlKα (1486.8 eV) 150W X-ray source, 0.5 mm circular spot size, a flood gun to counter charging effects, and the analysis chamber base pressure lower than 1×10^{-9} mbar, data were collected with FAT= 20 eV. X-ray diffraction. X-ray diffraction (XRD) data for **Cu_{22}-1** and **Cu_{22}-2** crystals were collected using Bruker D8 Advance diffractometer (Cu Kα). PXRD patterns of samples were collected at room temperature in air on a X'Pert PRO diffractometer (Cu-Kα). The element analysis was performed on Vario EL cube. 3 mg of each sample was used in the experiment.

1.4 X-Ray Crystallography

The data collections for single crystal X-ray diffraction were carried out on a Bruker Smart APEX II CCD diffractomete, using a a Cu-K radiation (λ=1.5418 Å). Data reductions and absorption corrections were performed using the SAINT and SADABS programs, respectively. The structure was solved by direct methods and refined with full-matrix least squares on F^2 using the SHELXTL software package. All non-hydrogen atoms were refined anisotropically, and all the hydrogen atoms were set in geometrically calculated positions and refined isotropically using a riding model.

1.5 Computational methods and details

Optimization of the geometric structures of Cu_{22}-1 and Cu_{22}-2 is achieved with the help of density functional theory (DFT) calculations in Dmol[3] package[1]. The Perdew-Burke-Erzerhof (PBE)[2, 3] functional

in the generalized gradient approximation (GGA) is applied in structural optimization. During the optimization process, the DFT semi-core pseudopotential approximation (DSPP)[4] and the DND[5] basis set including the *d* polarization function were used to deal with the inner electron and atomic orbitals of the cluster structure respectively. At the same time, Tkatchenko and Scheffler (TS)[6] dispersion correction is used in the optimization process. The convergence limits of the energy, energy gradient, and displacement of the geometric optimization are set to 1.0×10^{-5} Hartree, 4.0×10^{-3} Hartree/Å, and 5.0×10^{-3} Å, respectively.

The single point energies of two Cu_{22} were calculated using DFT at the PBE0-D3(BJ)[7, 8]/def2-TZVP[9] level, as implemented in the ORCA5.0.3 program system[10, 11]. TDDFT calculation is implemented using the ORCA software package at the level of PBE0[12]/def2-SV(P)[9]. In addition, the solvent effect was considered with 1, 2-dichloroethane in the SMD model[13]. The number of excited states calculated for each cluster is 300.

In order to reflect the differences in the electronic structures of Cu_{22}-1 and Cu_{22}-2, all the above calculations use the overall structure (without any simplification). Since the number of atoms in the two clusters is very large, we use the density-fitting approximation method to speed up the calculation of single-point energy and TDDFT (the error introduced is negligible). The density fitting basis set used is def2/J[14] (corresponding to the def2-SV(P) and def2-TZVP basis set, respectively). In addition, the data processing of PDOS and UV-Vis is implemented based on the Multiwfn3.8(dev) software package[15].

Reference

1. Delley, B., From molecules to solids with the DMol[3] approach. *The Journal of Chemical Physics* **2000,** *113* (18), 7756-7764.
2. Perdew, J. P.; Burke, K.; Ernzerhof, M., Generalized Gradient Approximation Made Simple. *Physical Review Letters* **1996,** *77* (18), 3865-3868.
3. Perdew, J. P.; Burke, K.; Ernzerhof, M., Generalized Gradient Approximation Made Simple. *Physical Review Letters* **1997,** *78* (7), 1396-1396.
4. Delley, B., Hardness conserving semilocal pseudopotentials. *Physical Review B* **2002,** *66* (15), 155125.
5. Delley, B., Ground-State Enthalpies: Evaluation of Electronic Structure Approaches with Emphasis on the Density Functional Method. *The Journal of Physical Chemistry A* **2006,** *110* (50), 13632-13639.
6. Tkatchenko, A.; Scheffler, M., Accurate Molecular Van Der Waals Interactions from Ground-State Electron Density and Free-Atom Reference Data. *Physical Review Letters* **2009,** *102* (7), 073005.
7. Grimme, S.; Antony, J.; Ehrlich, S.; Krieg, H., A consistent and accurate ab initio parametrization of density functional dispersion correction (DFT-D) for the 94 elements H-Pu. *The Journal of Chemical Physics* **2010,** *132* (15), 154104.
8. Grimme, S.; Ehrlich, S.; Goerigk, L., Effect of the damping function in dispersion corrected density functional theory. *Journal of Computational Chemistry* **2011,** *32* (7), 1456-1465.
9. Weigend, F.; Ahlrichs, R., Balanced basis sets of split valence, triple zeta valence and quadruple zeta valence quality for H to Rn: Design and assessment of accuracy. *Physical Chemistry Chemical Physics* **2005,** *7* (18), 3297-3305.
10. Neese, F., The ORCA program system. *WIREs Computational Molecular Science* **2012,** *2* (1), 73-78.
11. Neese, F., Software update: the ORCA program system, version 4.0. *WIREs Computational Molecular Science* **2018,** *8* (1), e1327.
12. Adamo, C.; Barone, V., Toward reliable density functional methods without adjustable parameters: The PBE0 model. *The Journal of Chemical Physics* **1999,** *110* (13), 6158-6170.

13. Marenich, A. V.; Cramer, C. J.; Truhlar, D. G., Universal Solvation Model Based on Solute Electron Density and on a Continuum Model of the Solvent Defined by the Bulk Dielectric Constant and Atomic Surface Tensions. *The Journal of Physical Chemistry B* **2009,** *113* (18), 6378-6396.
14. Weigend, F., Accurate Coulomb-fitting basis sets for H to Rn. *Physical Chemistry Chemical Physics* **2006,** *8* (9), 1057-1065.
15. Lu, T.; Chen, F., Multiwfn: A multifunctional wavefunction analyzer. *Journal of Computational Chemistry* **2012,** *33* (5), 580-592.

1.6 Two isomeric Cu_{22}-1 and Cu_{22}-2 catalyzed [3+2] azide–alkyne cycloaddition (AAC, click reaction).

Details of the catalytic procedure: Two separate 10 ml vials were chosen. The first vial was charged with **Cu_{22}-1** (0.06 mol%), benzyl azide (0.25 mmol, 1.0 equiv.), and phenylacetylene (0.3 mmol, 1.2 equiv.). The second vial was charged with **Cu_{22}-2** (0.06 mol%), benzyl azide (0.25 mmol, 1.0 equiv.), and phenylacetylene (0.3 mmol, 1.2 equiv.). Acetonitrile (2 ml) were added to both vials under a nitrogen atmosphere. The reaction mixtures were then irradiated with blue light (10-W blue light-emitting diode lamps). A cooling fan was used to maintain the reaction at room temperature, 28-30 °C) under N_2 (1 atm). A GC sample was taken from each vial and subjected to GC analysis to determine the product yield. All reactions were conducted under a nitrogen atmosphere in oven-dried glassware.

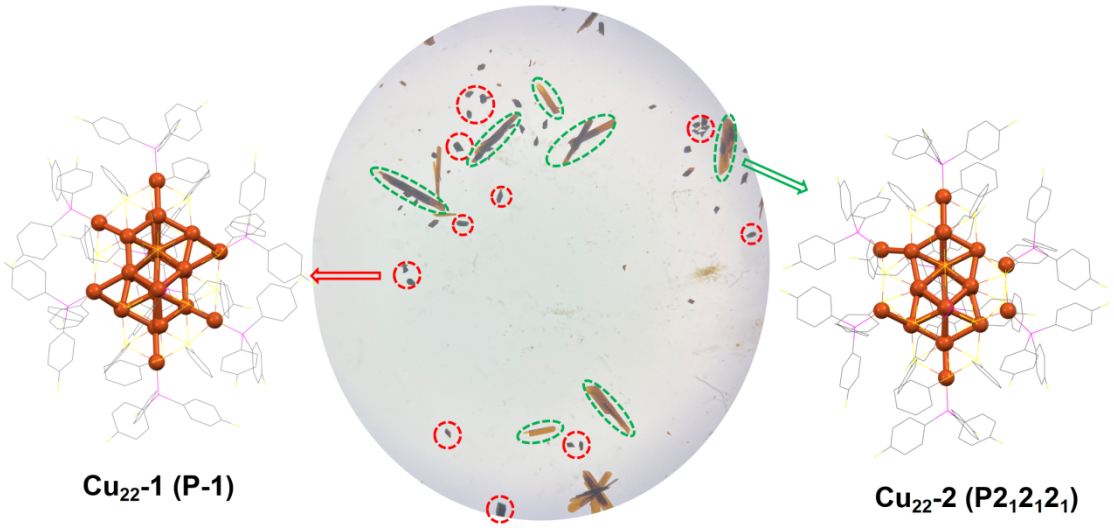

Figure S1. The digital photos of Cu_{22} nanoclusters.

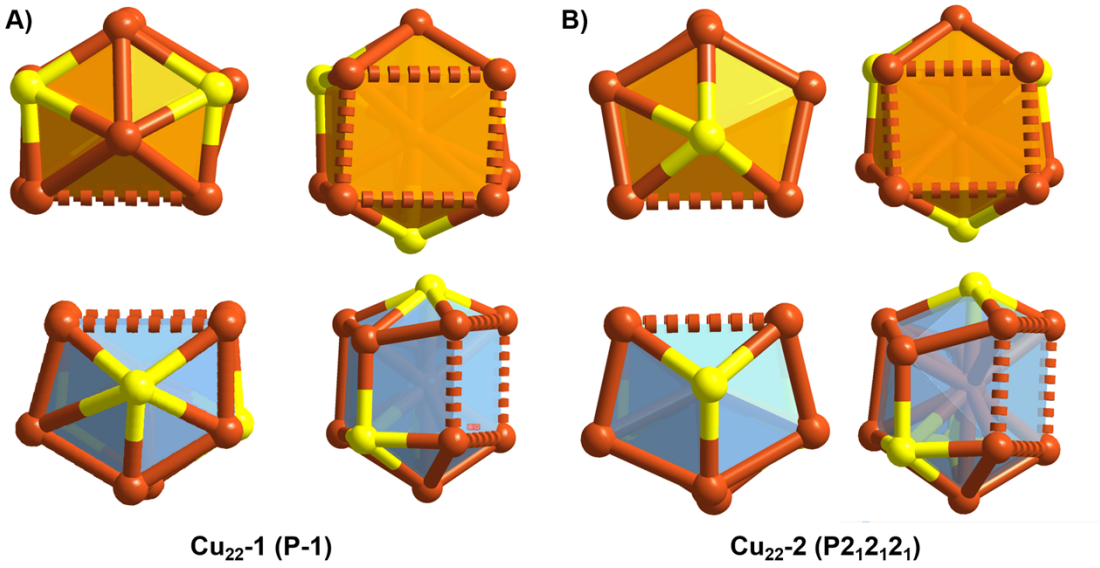

Figure S2. The two distorted Ino decahedron $Cu_{10}Se_3$ units.

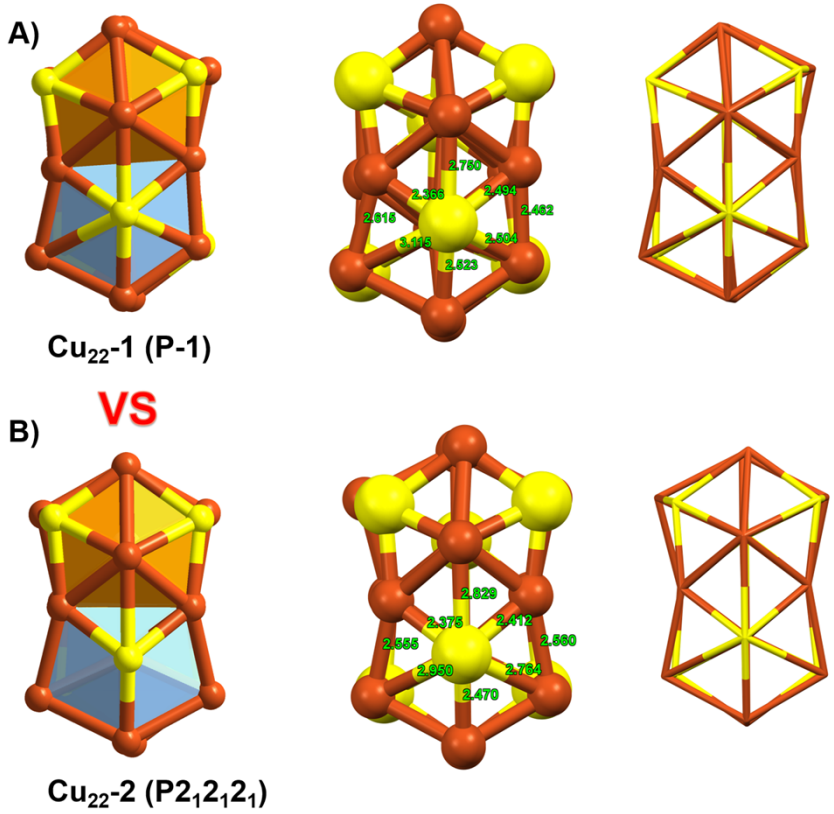

Figure S3. The comparison of two $Cu_{16}Se_6$ units of **Cu_{22}-1** and **Cu_{22}-2.**

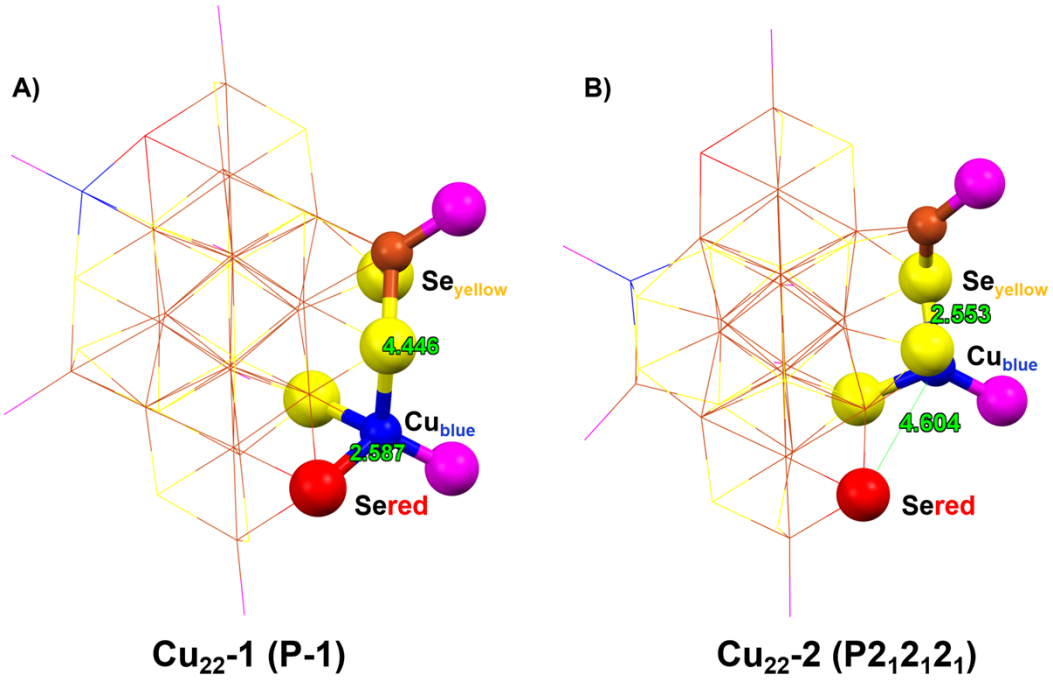

Figure S4. The detail comparison of bond distance of Cu_{blue}-Se_{red} and bond distance of Cu_{blue}-Se_{yellow}.

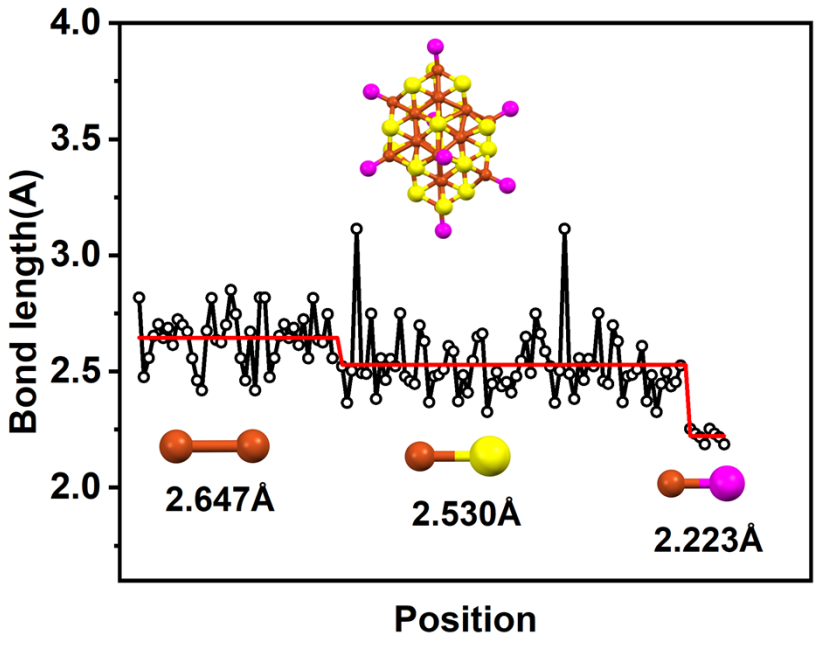

Figure S5. Bond lengths of the **Cu_{22}-1** nanocluster.

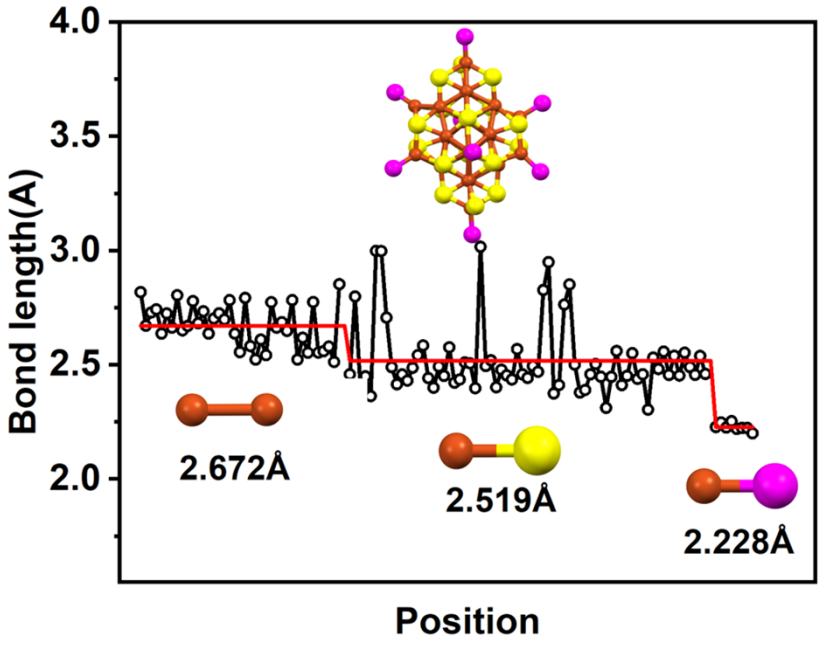

Figure S6. Bond lengths of the **Cu_{22}-2** nanocluster.

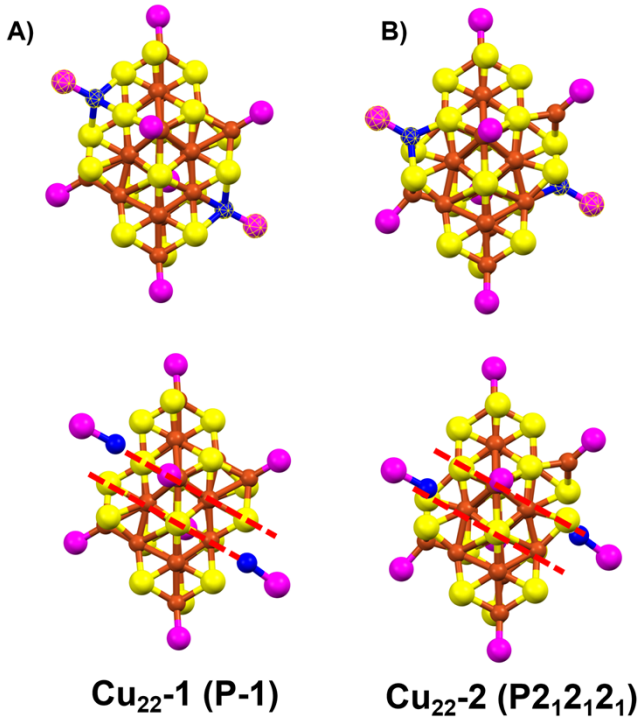

Figure S7. Differences in bonding modes between surface Cu-P ligands and the overall framework.

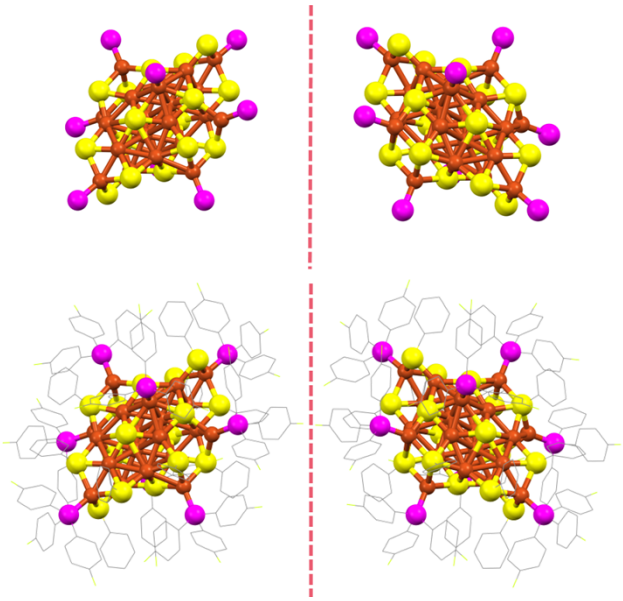

Figure S8. The enantiomers in the crystal unit cell of **Cu_{22}-2** ($P2_12_12_1$) .

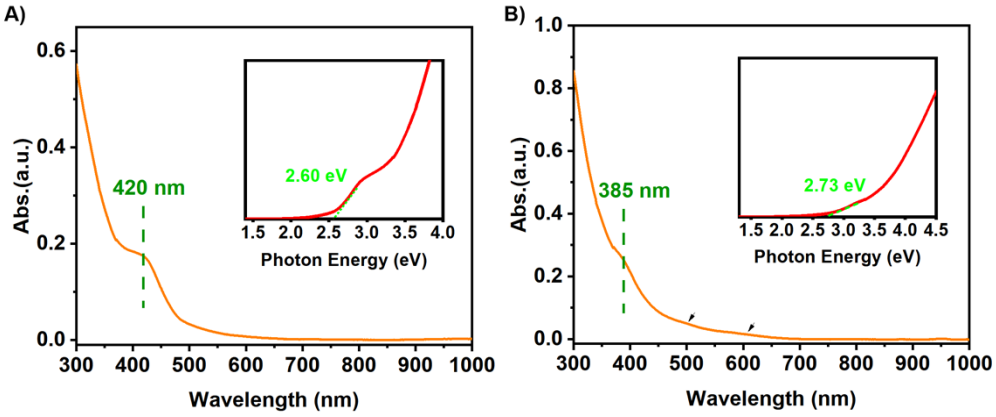

Figure S9. Optical absorption spectra and the spectra on the energy scale of A) **Cu_{22}-1** and B) **Cu_{22}-2**.

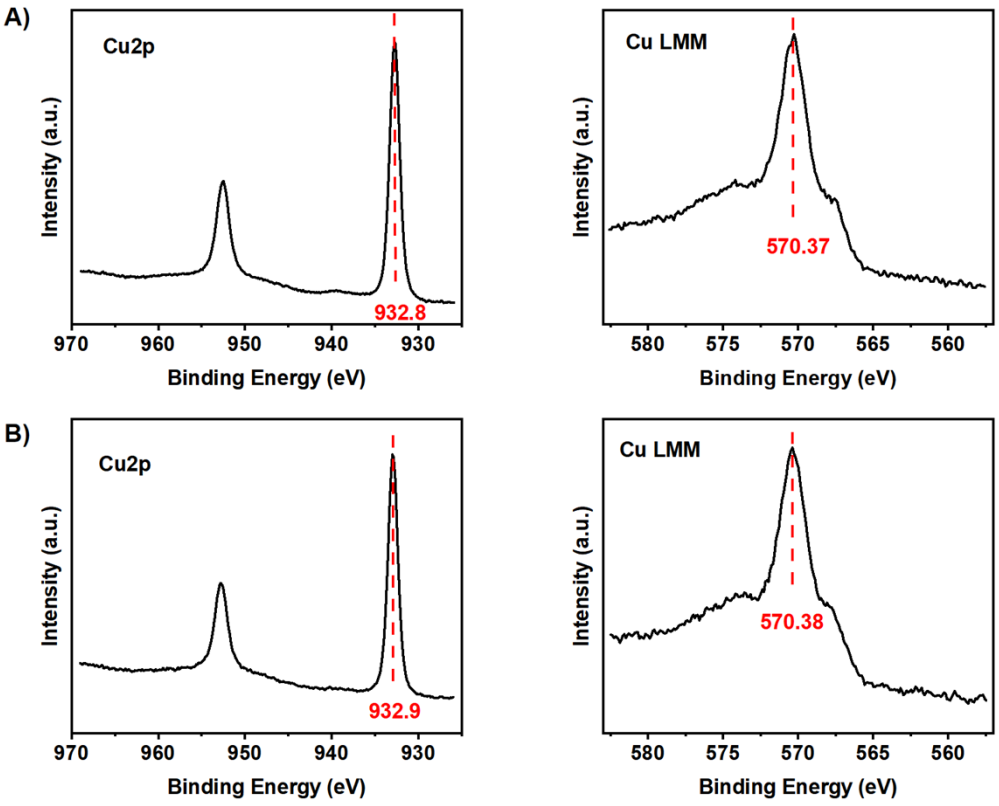

Figure S10. the XPS data of Cu2p and the Cu LMM spectra for A) **Cu_{22}-1** nanocluster and B) **Cu_{22}-2** nanocluster.

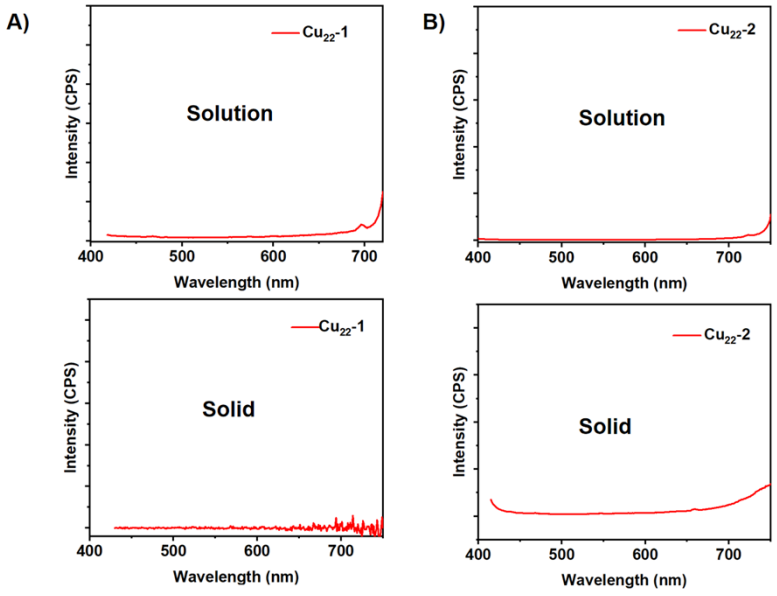

Figure S11. Emission Spectra of (A) **Cu_{22}-1** and (B) **Cu_{22}-2** in solution and solid states.

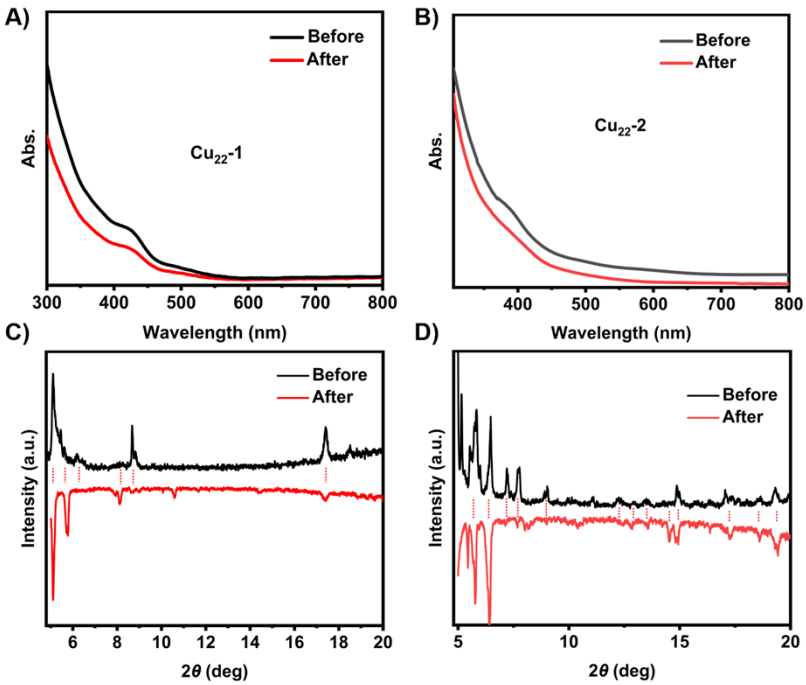

Figure S12. Stability test before and after catalysis. UV-vis spectra of (A) **Cu_{22}-1** and (B) **Cu_{22}-2** before and after catalysis. P-XRD spectra of (C) **Cu_{22}-1** and (D) **Cu_{22}-2** before and after catalysis.

Table S1. Crystal data and structure refinement for Cu22-1.

Identification code	ZHM-Cu22-1
Empirical formula	$C_{206}H_{150}Cl_4Cu_{22}F_{24}P_8Se_{16}$
Formula weight	6132.84
Temperature/K	120
Crystal system	triclinic
Space group	P-1
a/Å	17.7264(14)

b/Å	19.5316(15)
c/Å	19.7763(13)
α/°	117.328(5)
β/°	103.867(6)
γ/°	98.797(6)
Volume/Å^3	5624.4(8)
Z	1
Radiation	CuKα (λ = 1.54186)
2Θ range for data collection/°	7.732 to 138.922
Index ranges	-18 ≤ h ≤ 21, -23 ≤ k ≤ 13, -19 ≤ l ≤ 24
Reflections collected	51756
Independent reflections	20107 [R_{int} = 0.0169, R_{sigma} = 0.0219]
Data/restraints/parameters	20107/0/1261
Goodness-of-fit on F^2	1.031
Final R indexes [I>=2σ (I)]	R_1 = 0.0276, wR_2 = 0.0693
Final R indexes [all data]	R_1 = 0.0331, wR_2 = 0.0712
Largest diff. peak/hole / e Å^{-3}	1.47/-1.21

Table S2. Crystal data and structure refinement for Cu22-2.

Identification code	ZHM-Cu22-2
Empirical formula	$C_{204}H_{146}Cu_{22}F_{24}P_8Se_{16}$
Formula weight	5966.01
Temperature/K	120
Crystal system	orthorhombic
Space group	$P2_12_12_1$
a/Å	20.2077(6)

b/Å	29.3716(9)
c/Å	36.4328(12)
α/°	90
β/°	90
γ/°	90
Volume/Å^3	21624.1(12)
Z	4
Radiation	CuKα (λ = 1.54186)
2Θ range for data collection/°	11.688 to 139.118
Index ranges	$-10 \leq h \leq 24$, $-33 \leq k \leq 35$, $-35 \leq l \leq 44$
Reflections collected	94001
Independent reflections	37042 [R_{int} = 0.0437, R_{sigma} = 0.0595]
Data/restraints/parameters	37042/5676/2465
Goodness-of-fit on F^2	1.067
Final R indexes [I>=2σ (I)]	R_1 = 0.0677, wR_2 = 0.1697
Final R indexes [all data]	R_1 = 0.0757, wR_2 = 0.1737
Largest diff. peak/hole / e Å^{-3}	1.37/-0.87
Flack parameter	0.477(13)

Table S3. Elemental C, H contents measured by elemental analysis.

	Elemental analysis	
	Cal.	Exp.
Cu_{22}-1	C: 53.68%; H: 3.22%	C: 53.80%; H: 3.24%
Cu_{22}-2	C: 53.68%; H: 3.22%	C: 53.60%; H: 3.25%

Table S4. The attribution of the theoretically simulated UV-Vis absorption peak of Cu_{22}-1.

Cu_{22}-1	□	□	□	□
peak	**wavelength/nm**	**Excited state**	**Transition mode**	**Transition contribution/%**
α	605	1	H→ L	66.6
			H-1→ L	31.2
		2	H-1→ L	66.2
			H→L	31.0
β	485	5	H-5→L	88.2
γ	418	15	H→L+2	53.8
			H-11→L	13.1
		16	H-1→L+2	64.7
δ	366	30	H-17→L	35.6
			H-14→L	11.5
			H-1→L+4	11.2
		37	H-5→L+1	72.3
		56	H-1→ L+13	25.7
			H →L+15	14.5
		57	H-1→ L+14	25.5
			H→ L+14	20.8
□	□	□	H-1→ L+11	11.2

Table S5. The attribution of the theoretically simulated UV-Vis absorption peak of Cu_{22}-2.

Cu_{22}-2	□	□	□	□
peak	**wavelength/nm**	**Excited state**	**Transition mode**	**Transition contribution/%**
α	623	1	H → L	69.4
			H-1 → L	28.4
		2	H-1 → L	69.2

			H→ L	28.1
β	499	5	H-4→L	80.0
		6	H-8 → L	31.0
			H-9→ L	22.0
			H-6 →L	19.5
			H-7 →L	12.2
		7	H-7→L	54.5
			H-8→L	16.1
			H-5→L	10.7
γ	402	19	H-13→ L	22.4
			H-2 →L+1	16.6
			H →L+2	13.1
		21	H-3→ L+1	43.1
		22	H-1 → L+2	36.5
			H-1→ L+4	17.0
δ	367	36	H-7 →L+1	12.2
		37	H-7 →L+1	19.3
		41	H-20→L	22.9
			H-1→ L+3	10.0
		42	H→ L+8	10.2
		47	H-6→L+1	25.7
			H-19→ L	14.6
		48	H→ L+12	13.0
		50	H→ L+12	15.6
			H-1→L+7	13.2
		53	H-21→ L	12.4
		55	H→ L+13	16.4

			H-1 →L+9	14.7
θ	442	12	H-10→L	42.0
			H-13→ L	18.1
		14	H-12→L	36.4
			H-10→ L	19.9
□	□	□	H-11→L	16.8

Table S6. The catalytic performance of two isomeric **Cu_{22}-1** and **Cu_{22}-2**. [3+2] Cycloaddition between benzyl azide and phenylacetylene using isomeric **Cu_{22}-1** and **Cu_{22}-2** as catalyst under 50 °C oil bath.[a] Our study found that **Cu_{22}-1**'s catalytic activity stabilized at about 92% after 24 hours. Therefore, we also ended the reaction with **Cu_{22}-2** at the 24-hour mark to keep conditions consistent for comparison. This method allowed us to directly compare the catalytic performance of **Cu_{22}-1** and **Cu_{22}-2**. The similar catalytic effects suggest that the nanoclusters remain stable during the reaction.

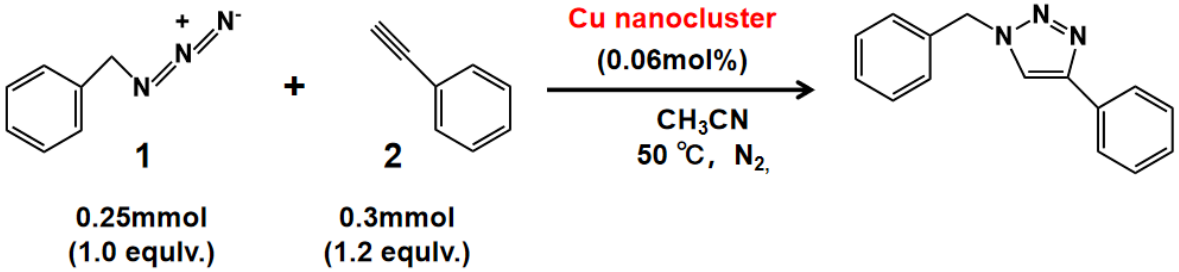

	The product yield determined by GC-MS (%)	
Catalyst[b]	**Cycle 1**	**Cycle 2**
Cu_{22}-1	**92 (24h); 80 (18h); 64 (12h)**	**89 (24h); 76 (18h); 60 (12h)**
Cu_{22}-2	**36(24h); 35 (18h); 32 (12h)**	**33(24h); 32 (18h); 30 (12h)**

[a] benzyl azide (0.25 mmol, 1.0 equiv.), phenylacetylene (0.3 mmol, 1.2 equiv.) and and acetonitrile (2 mL). [b] With respect to the amount of benzyl azide.